ISBN: 978-3-95450-208-0 doi:10.18429/JACoW-IPAC2019-WEPTS094

GENERATION HIGH-CHARGE OF FLAT BEAMS AT THE ARGONNE WAKEFIELD ACCELERATOR*

T. Xu[1†], G. Ha[2], M. Kuriki[3], P. Piot[1,4], J. G. Power[2], E. Wisniewski[2], M. Conde[2]
[1] Northern Illinois University, DeKalb, IL 60115, USA
[2]Argonne National Laboratory, Lemont, IL 60439, USA
[3]Hiroshima University, Higashi-Hiroshima, Japan 739-8557
[4]Fermi National Accelerator Laboratory, Batavia, IL 60510, USA

Abstract

Beams with large transverse emittance ratios (flat beams) have received renewed interest for their possible applications in future linear colliders and advanced accelerators. A flat beam can be produced by generating a magnetized beam and then repartitioning its emittance using three skew quadrupoles. In this paper, we report on the experimental generation of ~ 1 nC flat beams at the Argonne Wakefield Accelerator (AWA). The emittance ratio of the flat beam is demonstrated to be continuously variable by adjusting the magnetic field on the cathode.

INTRODUCTION

Flat electron beams with large transverse emittance ratios have various applications in conventional and advanced accelerators [1,2]. The generation of flat beams can be realized via a round-to-flat transformation of angular-momentum-dominated beams [3]. By immersing the cathode in a solenoidal field, electrons are produced with transverse correlation and asymmetric eigen-emittance. A subsequent skew quadrupole channel removes the correlation and restores the projected emittances to eigen-emittances. This round-to-flat beam transformation was experimentally demonstrated a decade ago and proposed as alternative to damping rings in linear colliders [4].

In this paper, we report on the commissioning of a beamline to produce flat beams at the AWA facility. The produced flat beam combined with the available transverse-to-longitudinal phase-space exchanger [5–7] is expected to open new opportunities in arbitrary emittance repartitioning within the three degrees of freedom. The use of high-charge (nC) flat beams in beam-driven wakefield accelerator are expected to mitigate transverse instabilities in planar slow-wave structures [8]. Finally, the produced flat beam will also support experiments related to plasma-based lenses [9].

THEORY AND METHODS

The theory of round-to-flat transformation was detailed in Ref. [1, 3, 10]. In brief, when a strong axial magnetic field is applied on cathode, electrons are born carrying magnetization which sets eigen-emittance partition. It is given by $\mathcal{L} = \frac{eB_c}{2mc}\sigma_c^2$, where we refer to $\mathcal{L}$ as the magnetization. B_c is the axial magnetic field on the photocathode surface and σ_c the rms transverse size. Considering a "magnetized" (or canonical-angular-momentum (CAM)-dominated) beam $\mathcal{L} \gg \varepsilon_{\rm u}$ (where $\varepsilon_{\rm u}$ refers to uncorrelated emittance), the eigen-emittances $\varepsilon_\pm$ are unequal and given by:

$$\varepsilon_{n,+} = 2\gamma\mathcal{L}, \text{and } \varepsilon_{n,-} = \frac{\varepsilon_{n,u}^2}{2\gamma\mathcal{L}},$$

where γ is the Lorentz factor and $\varepsilon_{n,u} \equiv \gamma\varepsilon_u$. These eigen-emittances can be mapped to conventional emittances $\varepsilon_{\rm x,y}$. In such a round-to-flat-beam transformation (RFBT), the incoming cylindrically-symmetric CAM-dominated beam is converted to a flat beam with emittance ratio $\varrho = \varepsilon_{n,+}/\varepsilon_{n,-}$. A simple impementation of an RFBT beamline consists of three skew-quadrupole magnets [1]. The quadrupole magnets settings can be found by solving the matrix equation $A(I-C) = B(I+C)$, where A and B are 2×2 transfer matrix of an unskewed RFBT in respectively the $\widetilde{\mathbf{X}} \equiv (x, x')$ and $\widetilde{\mathbf{Y}} \equiv (y, y')$ phase spaces, I is the identity matrix, and C is the correlation matrix defined by $\mathbf{Y} = C\,\mathbf{X}$. This matrix C can be statistically computed as $C \equiv \langle\mathbf{Y}\widetilde{\mathbf{X}}\rangle\langle\mathbf{X}\widetilde{\mathbf{X}}\rangle^{-1}$ where $\langle\mathbf{X}\widetilde{\mathbf{X}}\rangle$ and $\langle\mathbf{Y}\widetilde{\mathbf{X}}\rangle$ are 2×2 blocks of the 4×4 covariance matrix Σ associated to the $(\mathbf{X},\mathbf{Y})$ transverse phase space. Given the general form of the Σ matrix derived in [3], we find the general form of C to be

$$C = \frac{\gamma\mathcal{L}}{\varepsilon_n}\begin{pmatrix} \alpha & \beta \\ -\frac{1+\alpha^2}{\beta} & -\alpha \end{pmatrix}, \quad (1)$$

where (α,β) and $\varepsilon_n = [\varepsilon_{u,n}^2 + (\gamma\mathcal{L})^2]^{1/2} \simeq \gamma\mathcal{L}$ are respectively the Courant-Snyder (C-S) parameters and normalized emittance associated with the CAM-dominated beam. For a CAM-dominated beam the factor $\gamma\mathcal{L}/\varepsilon_n \simeq 1$ so that the correlation matrix is conveniently described by the C-S parameters only and its determinant is $\det(C) \simeq 1$. Under the thin-lens approximation, the skew-quadrupole-magnet settings are analytical functions of the elements of C [11].

AWA BEAMLINE & SIMULATIONS

The AWA drive-beam accelerator is diagrammed in Fig. 1. The beamline incorporates a 1+1/2 L-band (1.3 GHz) RF gun followed by six 7-cell cavities (Ci). The RF-gun cavity is surrounded by three solenoidal lenses. The bucking and focusing solenoid (LB and LF) are nominally powered in

* This work was supported by the US Department of Energy (DOE) contracts # DE-SC0018656 and # DE-SC0018234 (U.S.-Japan Science & Technology Cooperation Program in High Energy Physics) with NIU and No.DE-AC02-06CH11357 with ANL.
† xu@niu.edu

ISBN: 978-3-95450-208-0 doi:10.18429/JACoW-IPAC2019-WEPTS094

series so to cancel the magnetic field on the cathode surface. In our studies, LB was turned off so that the magnetic field on the cathode is controlled by LF. A matching solenoid (LM) provides further control on the beam size and emittance. Linac C4 and C6 are turned off in our experiment. The RFBT beamline consists of the skew quadrupole magnets (DQ1-3). The RFBT is followed by quadrupole magnets (Q1-4). The available diagnostics include YAG:Ce scintillating screens (YAG4-7) along with a set of horizontal and vertical scanning slit at the YAG5 diagnostic station. The typical beamline parameters used during our experiments and simulations are summarized in Table 1.

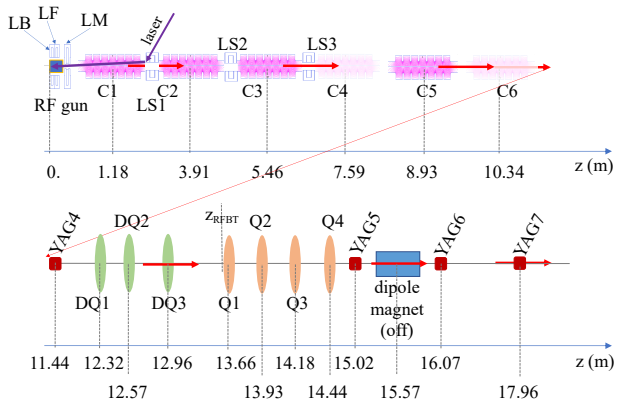

Figure 1: Diagram of the AWA drive-beam photoinjector beamline. The labels “C", “L", “DQ" and “Q" refer respectively to accelerating cavities, solenoidal lenses, skew-quadrupole magnets, and quadrupole magnets. The "YAG" labels indicate the locations of diagnostics stations.

Table 1: Accelerator Parameters for Subsystem Pertinent to the Generation of CAM-dominated Beams

Parameter	Value	units
Laser pulse duration FWHM	8	ps
Laser spot radius	3.2	mm
Laser launch phase	50	deg
Magnetic field on cathode (B_c)	0.125	T
Beam energy	43	MeV
Magnetization ($\gamma\mathcal{L}$)	102	µm

In order to assess the performance of the flat-beam generation at AWA, beam-dynamics simulations were performed using the IMPACT-T program. The beam dynamics was performed in two stages. First, the beamline parameter (laser, gun, linacs, solenoids) were optimized to minimize the uncorrelated emittance $\varepsilon_{n,u}$ while maximizing the eigen-emittances ratio ϱ downstream of the linac at $z = 11$ m. As shown in Fig. 2, the optimizations indicate that the solenoid LM plays a critical role in the emittance-compensation process while LF sets the magnetization. We also find that lower $\varepsilon_{n,u}$ are attained as the magnetization increases. The optimized phase-space distributions for a CAM-dominated beam are then transformed into flat beams. The settings of quadrupole magnets DQ1-3 obtained from different methods are summarized in Table 2. Generally, we find that a simple numerical optimization using a thick-lens transfer-matrix model is sufficient to devise the skew-quadrupole-magnet settings (they give similar results than lengthier optimization performed with IMPACT-T). It should be noted that given the limited field gradient ($B' \leq 7$ T/m) available from the DQ1-3 magnets, the linac solenoids LS2, and LS3 are used to control the C-S parameters (α, β) in Eq. (1). The simulations generally demonstrate that high charge (1 nC) beams with emittance partitions $\varepsilon_+, \varepsilon_- = (180, 0.2)$ µm could be attained at AWA.

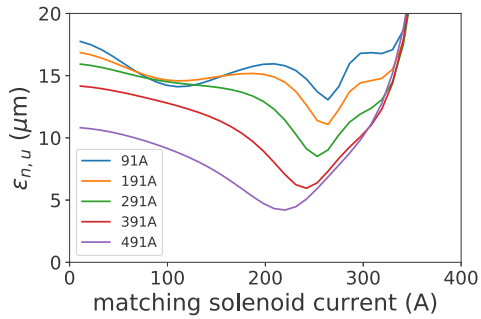

Figure 2: IMPACT-T simulation of $\varepsilon_{n,u}$ versus LM current. The different trace corresponds to different LF settings.

Table 2: Skew Quad Settings for a Simulated Configuration ($\alpha = 0$, $\beta = 1.5$m)

Methods	Thin-lens	Thick-lens	IMPACT-T
DQ1 B' (T/m)	5.793	4.079	4.004
DQ2 B' (T/m)	-7.315	-5.091	-5.063
DQ3 B' (T/m)	8.751	4.471	4.563

EXPERIMENTAL METHODS & RESULTS

As discussed, the generation of flat beams requires a precise knowlege of the parameters associated with the incoming CAM-dominated beam. Likewise, producing a flat beam with minimized 4D emittance relies on properly tuning the LS2 and LS3 solenoids.

In order to experimentally characterize the CAM-dominated beam we measure the magnetization $\mathcal{L}$ is measured with the slit method [12], We insert a, e.g. vertical, slit at YAG5 and observe the rotation angle θ of transmitted beamlet at YAG7. Given the YAG5-YAG7 distance D and the measurement of the full-beam size at YAG5 and YAG7 ($\sigma_{5,7}$), the magnetization can be inferred from $\mathcal{L} = \frac{\sigma_5\sigma_7 \sin\theta}{D}$. Note that for a CAM-dominated beam $\mathcal{L}$ plays the role of the emittance. Likewise the C-S parameters is measured by fitting the drift-space envelope equation evolution $\sigma(z; \beta_0, z_0) = \sqrt{\beta_0\mathcal{L}[1 + (\frac{z-z_0}{\beta_0})^2]}$ to the beam size measured in the x and y directions at YAG4-7. The the fitting parameters are the betatron function at the waist β_0, and

ISBN: 978-3-95450-208-0 doi:10.18429/JACoW-IPAC2019-WEPTS094

the waist location z_0. The C-S parameter can then be propagated to the RFBT entrance z_{RFBT} via $\beta = \beta_0 + \frac{(z_{\mathrm{RFBT}}-z_0)^2}{\beta_0}$ and $\alpha = -\frac{2(z_{\mathrm{RFBT}}-z_0)}{\beta_0}$. The latter procedure gives us the C matrix 1 at z_{RFBT} which can then be used to devise the settings of DQ1-3. Once the flat beam is generated, its emittances are measured using a scanning-slit technique [13]. For each slit position, an average of 30 frames is recorded and the associated projections are fitted with a Gaussian distribution. The reconstructed phase space is shown in 3. The measured emittances and reconstructed phase space of a 1 nC flat beam appear respectively in Table 3 and Fig. 3. We generally are able to produce large emittance ratios $\varrho \geq 100$ with larger emittance consistent with the expected value $2\gamma\mathcal{L}$. However, the small-emittance is measured to be higher than the simulated value. The discrepancy is currently attributed to an imprecise optimization of the LM solenoid to minimize $\varepsilon_{n,u}$ or its possible deterioration due to time-dependent kicks imparted by the RF input-power couplers in the low-energy section of the linac.

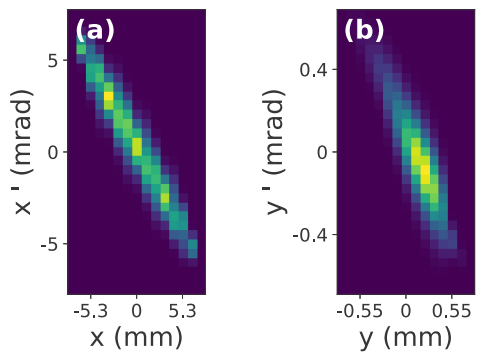

Figure 3: Reconstructed horizontal (a) and vertical (b) phase space at YAG5 associated with a 1 nC flat beam.

Table 3: Comparison of Measured and Simulated Flat-beam Parameters

Parameter	**Value**	
Bunch charge (nC)	1.0±0.18	
$\varepsilon_+ = \varepsilon_x$ (μm)	213.20±31.9	
$\varepsilon_- = \varepsilon_y$ (μm)	1.93±0.28	
emittance ratio	110	
Skew quads	**measured**	**simulated**
DQ1 B' (T/m)	-3.13	-3.26
DQ2 B' (T/m)	3.93	3.97
DQ3 B' (T/m)	-3.23	-3.13

In the second set of experiment, we vary the magnetic field on cathode B_c using LF and measured the produced flat-beam emittances. For this experiment we reuse the same DQ1-3 settings optimized for the 1 nC charge (see Table 3) and, for each value of LF, we used the solenoid LM and LS3 to minimize the uncorrelated emittance and rematch the beam in the RFBT. The corresponding flat-beam distribution and parameters are respectively compared in Fig. 4 and Table 4.

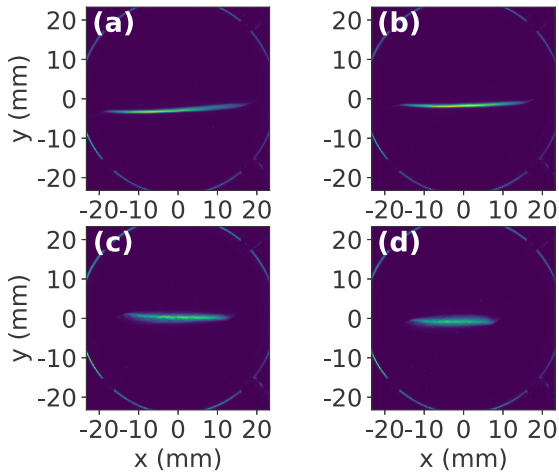

Figure 4: Measure flat-beam (x, y) distribution at YAG7 for LF current (A) of 491 (a), 391 (b), 291 (c) and 191 (d).

Table 4: Flat-beam Parameters Measured for Different B_c

Current (A)	491	391	291	191
B_c(T)	0.125	0.1	0.074	0.049
Charge (nC)	0.63 ±0.05	0.63 ±0.06	0.74 ±0.14	0.5 ±0.1
ε_+ (μm)	215.6 ±32.3	175.2 ±26.2	136.4 ±20.4	77.3 ±11.5
ε_- (μm)	1.4 ±0.2	1.1 ±0.2	1.9 ±0.3	1.4 ±0.2
$\varepsilon_+\varepsilon_-$ (μm^2)	306.9	186.9	270.0	108.3
emittance ratio	152	164	69	55

As anticipated the LF solenoid controls the flat-beam emittance ratio with the trend that increasing values of B_c generally correspond to larger emittance ratios ϱ. Further work is needed to minimize the uncorrelated emittance. Nevertheless, our work demonstrated that simply tuning two solenoids (LM and LS2) provided a way to vary the emittance partition between the two transverse degrees of freedom.

CONCLUSION

In summary, we have commissioned a round-to-flat beam transformer at AWA. The beamline is capable of producing flat beams with variable emittance ratios. The coupling of the RFBT to a transverse-to-longitudinal phase-space exchanger is expected to provide new electron-beam-tailoring capabilities. Our future work will combine these two beamlines to explore the control of emittance partition within the three degrees of freedom. Likewise, the high-charge flat beams are foreseen to have applications to some advanced acceleration concepts.

ISBN: 978-3-95450-208-0 doi:10.18429/JACoW-IPAC2019-WEPTS094

REFERENCES

[1] R. Brinkmann, Y. Derbenev, and K. Flöttmann, "A low emittance, flat-beam electron source for linear colliders," *Phys. Rev. Spec. Top.–Accel. Beams*, vol. 4, p. 053501, May 2001.

[2] A. Ody, P. Musumeci, J. Maxson, D. Cesar, R. England, and K. Wootton, "Flat electron beam sources for DLA accelerators," *Nucl. Instrum. Methods Phys. Res., Sect. A*, vol. 865, pp. 75–83, Sept. 2017.

[3] K.-J. Kim, "Round-to-flat transformation of angular-momentum-dominated beams," *Phys. Rev. Spec. Top.–Accel. Beams*, vol. 6, p. 104002, Oct. 2003.

[4] P. Piot, Y.-E. Sun, and K.-J. Kim, "Photoinjector generation of a flat electron beam with transverse emittance ratio of 100," *Phys. Rev. Spec. Top.–Accel. Beams*, vol. 9, p. 031001, Mar. 2006.

[5] P. Emma, Z. Huang, K.-J. Kim, and P. Piot, "Transverse-to-longitudinal emittance exchange to improve performance of high-gain free-electron lasers," *Phys. Rev. Spec. Top.–Accel. Beams*, vol. 9, p. 100702, Oct. 2006.

[6] P. Piot, Y. Sun, J. Power, and M. Rihaoui, "Generation of relativistic electron bunches with arbitrary current distribution via transverse-to-longitudinal phase space exchange," *Phys. Rev. Spec. Top.–Accel. Beams*, vol. 14, p. 022801.

[7] G. Ha, M. Cho, W. Namkung, J. Power, D. Doran, E. Wisniewski, M. Conde, W. Gai, W. Liu, C. Whiteford, Q. Gao, K.-J. Kim, A. Zholents, Y.-E. Sun, C. Jing, and P. Piot, "Precision Control of the Electron Longitudinal Bunch Shape Using an Emittance-Exchange Beam Line," *Phys. Rev. Lett.*, vol. 118, p. 104801, Mar. 2017.

[8] S. Baturin, G. Andonian, and J. Rosenzweig, "Analytical treatment of the wakefields driven by transversely shaped beams in a planar slow-wave structure," *Phys. Rev. Accel. Beams*, vol. 21, p. 121302, Dec. 2018.

[9] J. Rosenzweig. UCLA, personal communication.

[10] Y. Derbenev, "Adapting Optics for High Energy Electron Cooling," *University of Michigan Report No. UM- HE-98-04*, 1998.

[11] E. Thrane, C. Bohn, N. Barov, D. Mihalcea, Y. Sun, K. Bishofburger, D. Edwards, H. Edwards, S. Nagaitsev, J. Santucci, *et al.*, "Photoinjector Production of A Flat Electron Beam," in *Proc. 21st Linear Accelerator Conf.*, (Gyeongju, Korea), p. 308, 2002.

[12] Y.-E. Sun, P. Piot, K.-J. Kim, N. Barov, S. Lidia, J. Santucci, R. Tikhoplav, and J. Wennerberg, "Generation of angular-momentum-dominated electron beams from a photoinjector," *Phys. Rev. Spec. Top.–Accel. Beams*, vol. 7, p. 123501, Dec. 2004.

[13] M. Zhang, "Emittance formula for slits and pepper-pot measurement," Tech. Rep. FNAL-TM–1988, 395453, Fermi National Accelerator Lab, Oct. 1996.